Magazine of Civil Engineering

ISSN 2712-8172

journal homepage: http://engstroy.spbstu.ru/

Research article

UDC 691.335

DOI: 10.34910/MCE.115.3

Water treatment residue and coal fly ash geopolymers

***Q.M. Do*[1], *H.U.P. Nguyen*[1], *V.Q. Le*[2], *M.D. Hoang*[3]** ✉

[1] *Ho Chi Minh City University of Technology – Vietnam National University, Ho Chi Minh City, Vietnam*

[2] *Vietnam Institute for Building Materials, Hanoi, Vietnam*

[3] *Vietnam Institute for Building Science and Technology, Hanoi, Vietnam*

✉ *hmduc@yahoo.com*

Keywords: water treatment residue, coal fly ash, analcime, geopolymer, autoclave curing

Abstract. Water treatment residue (WTR) from water purification is a non-hazardous solid waste commonly discharged in landfills. WTR contains aluminosilicates and can participate in geopolymerization. Due to the low alkaline activity of WTR, we used coal fly ash with the WTR to coal fly ash ratio from 80 wt% to 50 wt% and activated it with the 8M NaOH solution. The specimens were cured in normal conditions for 28 days at room temperature, and in an autoclave for 7 days under a pressure of 2 MPa and temperature of 215 ºC. The test results showed that the compressive strength of geopolymers cured in an autoclave reached 28.8 MPa, which is much higher than for those cured in normal conditions with only 13.2 MPa. The microstructure (XRD, SEM) and chemical bonding (FTIR) analyses confirmed the analcime crystal formation in the geopolymers.

Acknowledgment. We appreciate the time and facilities provided by the Ho Chi Minh City University of Technology (HCMUT), VNU-HCM, for this study.

Citation: Do, Q.M., Nguyen, H.U.P., Le, V.Q., Hoang, M.D. Water treatment residue and coal fly ash geopolymers. Magazine of Civil Engineering. 2022. 115(7). Article No. 11503. DOI: 10.34910/MCE.115.3

1. Introduction

Water treatment residue (WTR) is waste obtained from water purification plants. The solid waste is not hazardous, but discharging it into a landfill requires a large land area and is an environmental challenge. Over the years, there have been many studies on using WTR in the production of building materials. WTR is used to partially replace clay in the production of bricks and ceramics [1-5], lightweight aggregates [6–8], and cement [9–11]. WTR can also be used as a mineral admixture [12–16] in cement concrete. Another promising application is the use of WTR in the production of alkali-activation materials (AAM) or geopolymer [17–22].

AAM is a cement-like material obtained by the reaction between an aluminosilicate precursor and an alkaline activator. Initially, the aluminosilicate precursor dissolves in an alkaline solution to form free SiO_4 and AlO_4 units. Then, the reaction between them under alkaline conditions produces a hydrous alkaline-aluminosilicate and/or alkali-alkali earth-aluminosilicate phase [23]. The formation can be described as a polymer-like condensation process, where the loss of water between two hydroxyl groups occurs in inorganic materials, and the materials can be named "geopolymers" [24]. The geopolimerization starts with oligomer condensation into a small ribbon-like molecule.

Several industrial byproducts and wastes, including WTR, blast furnace slag, rice husk, CFA, mining waste, and steel slag, can be used as aluminosilicate precursors to produce AAM. Alkaline-activated

solutions are mainly composed of alkalis of sodium or potassium and water glass. The aluminosilicate or silica precursors are dissolved in the alkaline-activated solution to create alkaline solutions. The condensation process of this alkaline solution forms geopolymer materials. Of course, if the condensation process does not occur, a geo-material does not form. The problem resulting from this reaction is that the alkali cations (K^+ and Na^+) are outside the polymerization network's structure. These cations can freely migrate in contact with water generating leaches to increase pH and low long-term characteristics.

One of the important characteristics of geopolymers is the presence of zeolites. The presence of analcime crystals in various ancient cements confirms that this zeolite is a stable, final stage of the long thermal transition of zeolitic materials [26]. The proportion of oxides participating in the $M_n[-(SiO_2)_z - AlO_2]_n \cdot mH_2O$ bonding chain affects the bonding strength. MacKenzie et al. [27] reported that the optimal molar ratios are in the range of $SiO_2/Al_2O_3 < 3.3$, $H_2O/Na_2O < 10$, and $Na_2O/SiO_2 < 0.3$. During geopolymerization, when the zeolites crystallize, the formation of the zeolite with different structures depends on the Si/Al ratios used. The higher the silicate content, the more analcime crystals can be obtained [28].

Hydrothermal curing at high temperatures and pressure are better than atmospheric conditions for analcime to crystallize and develop. Yuan-yuan Ge et al. reported a simple method to fabricate large-size single analcime crystals using the geopolymer-gels-conversion method. The crystal's architecture is icositetrahedron with a diameter range from 50 μm to 1200 μm. It also shows that the analcime's synthesis of single crystals depends on the hydrothermal time [28]. Kupwade-Patil and Allouche investigated the alkali silica reaction between reactive aggregates and the geopolymer matrix. They used one class C and two class F fly ashes to produce the geopolymer matrix and found the analcime crystals [29]. A high molar ratio of Na_2O/SiO_2 in the activated solution or low Si/Al molar ratio in aluminosilicate precursors tend to produce loose particles (pseudo-zeolitic structure, mainly Q4) rather than continuously well-connected NASH gel [24, 26, 30]. The rational content of the silicates is essential to form a compact alkali-aluminosilicate geopolymer with continuous gels, especially for aluminosilicate precursors with a lower Si/Al ratio [31].

WTR contains silicone and aluminum oxides, which hardly dissolve in alkaline solutions. Thus, it is not possible to use WTR alone for geopolymer production. In this case, the additional aluminosilicate precursors like fly ash (FA), rice husk ash (RHA), ground granulated blast furnace slag (GGBFS), or metakaolin (MK) play an important role. Waijarean N. et al. reported that the WTR was activated by heating in an electric furnace at 800 °C for 1 hour and fine grinding. At the same heating temperature, the aluminosilicate in WRT can be transferred to MK. In addition, we can use rice husk to adjust the molar SiO_2/Al_2O_3 ratio of the mix from 1.78 to 2.00 [32]. In similar experiments, the WTR mixture with 10M NaOH was heated at 800 °C for 1 h to create a geopolymer. The molar ratios of the geopolymer were $Na_2O/SiO_2 = 0.28$, $SiO_2/Al_2O_3 = 1.78$, $H_2O/Na_2O = 11.11$ and $H_2O/Al_2O_3 = 9.67$ [22].

Geraldo et al. used sodium silicate solution ($Na_2O.nSiO_2.mH_2O$) and sodium hydroxide (NaOH) as the alkaline activator. The alkali source was an alternative sodium silicate solution made from a mixture of NaOH and RHA. MK was partially replaced by WTR in the proportions of 0 wt%, 15 wt%, 30 wt%, and 60 wt%. The additional RHA was used in the geopolymer mixtures to keep SiO_2/Al_2O_3 molar ratio constant. Geopolymer mortars were cured at room temperature and had a compressive strength of 25 MPa at 28 days corresponding to a replacement ratio of 15% [17].

Using sodium silicate solution (Na_2SiO_3) and NaOH solution in a Na_2SiO_3/NaOH 80:20 mass ratio is considered optimal for all tests of Suksiripattanapong C. et al. [33]. The WTR-CFA geopolymers were dried at 75 °C, 85 °C, and 95 °C for 72 hours. The strength of WTR-CFA geopolymers dried at 75 °C, 85 °C, and 95 °C for 72 hours was 20 MPa, 18 MPa, and 16 MPa, respectively, meeting the strength requirements for bearing masonry units according to the Thai Industrial Standard.

A recent study on AAM from red mud and fly ash [34] showed that curing at high temperatures and high pressure in an autoclave increased the solubility of oxides and accelerated the reaction. AAM mixture of 26.3 wt% fly ash and 73.7 wt% red mud, activated by a 1M NaOH solution, reaches a strength of up to 20 MPa and a softening coefficient of more than 0.90.

In this study, we propose a treatment option for WTR of water purification plants in Vietnam as unfired building materials. WTR was used with CFA to produce geopolymer by autoclave technology at high temperatures and pressure. Unlike most previous studies that use the oxides content of raw materials to calculate the $SiO_2/Al2O_3$ molar ratio, we used the dissolved fraction in NaOH solution with different concentrations. This study focused on the compressive strength and microstructure characteristics of geopolymer with different WTR ratios cured in normal and autoclaved conditions.

2. Materials and Methods

2.1. Materials

Raw materials for the geopolymer were the WTR disposal of the Thu Duc water purification plant (Ho Chi Minh City, Vietnam) and the CFA (class F) of the Vinh Tan thermal power plant (Binh Thuan, Vietnam). The chemical compositions were detected using X-ray fluorescence (XRF) analysis. The physical properties are given in Table 1 and Table 2, respectively.

Table 1. Chemical compositions of raw materials.

Material	Oxides content, wt.%									
	SiO_2	Al_2O_3	Fe_2O_3	P_2O_5	Na_2O	K_2O	CaO	TiO_2	Other	LOI
WTR	32.8	26.3	33.7	0.223	-	0.126	1.91	3.59	0.967	6.38
CFA	48.93	26.19	11.22	-	-	6.94	1.52	1.38	2.27	1.55

Table 2. Physical properties of raw materials.

Material	Moisture content, wt%	Bulk density, kg/m^3	Density, g/cm^3	Mean particle size, μm
WTR	5.11	565	2.61	29.9
CFA	0.1	595	2.20	45.5

2.2. The alkaline activity of oxides

We used the solubility in an alkaline solution to estimate the alkaline activity of oxides in raw materials. The active oxides dissolved and reacted with alkaline according to the following equations (1 and 2):

$$SiO_2.nH_2O + 2NaOH = Na_2SiO_3 + (n + 1)\ H_2O \quad (1)$$

$$Al_2O_3.nH_2O + 2NaOH = 2NaAlO_2 + (n + 1)\ H_2O \quad (2)$$

We dried the WTR or CFA at 120°C to constant mass. Then, we put 25 g of the dried WTR or CFA and 25 ml of xM (where x is a molar index) NaOH solution into a stainless-steel bomb. The bomb was tightly screwed and placed in the oven at (80 ± 2) °C for 24 hours. After that, we cooled it down to room temperature. We filtered the sample in the flask and collected the filtrate in the test tube. The solution was filtered to determine the content of dissolved silicon, iron, and aluminum oxides (Table 3).

Table 3. Dissolved oxides content in an alkaline solution of different concentration.

Items		Dissolved oxides content, wt% at a concentration of alkaline activators of								
		1M	2M	3M	4M	5M	6M	7M	8M	9M
WTR	SiO_2	0.46	0.71	0.90	1.10	1.35	1.67	1.89	2.06	2.24
	Al_2O_3	1.56	3.08	3.21	4.47	5.42	6.51	7.59	8.90	20.12
	Fe_2O_3	0.03	0.03	0.05	0.07	0.09	0.13	0.17	0.19	0.20
CFA	SiO_2	2.33	3.34	4.58	6.78	8.66	9.34	10.65	12.06	13.68
	Al_2O_3	4.56	4.66	4.66	4.69	4.70	4.72	4.76	4.76	4.76

Test results in Table 3 show the acceleration of the dissolution process of oxide in raw materials while increasing the alkaline activator concentration. An interesting phenomenon observed is the dissolved content of aluminum oxide of WTR increases from 1.56 % to 20.12 % while increasing the NaOH concentration from 1M to 9M. Meanwhile, it varies in a narrow range of (4.56–4.76) % in the case of CFA.

The dissolved content of silicon oxide in both WTR and CFA increases proportionally with the NaOH concentration from 1M to 9M. But the dissolved content of silicon oxide of WTR, even in 9M NaOH solution (2.24 %), is less than that of CFA in 1M NaOH solution (2.33 %). This result explains the essential role of CFA in geopolymer formation in the WTR-CFA system.

2.3. Specimen preparation

We mixed the dried WTR and CFA powder at a predetermined weight ratio (GP-1, GP-2, GP-3, and GP-4). After that, the NaOH 8M solutions were added to mixtures at the weight ratio of the NaOH solution to (WTR+CFA) equal to 0.15, as shown in Table 4.

Table 4. Mix proportion and curing condition.

Sample	WTR/CFA, wt%	NaOH/(WTR+CFA), wt%	Curing condition	
			Atmosphere	Autoclave
GP-1	80	0.15	28 days, room temperature	2 MPa, 7 h
GP-2	75	0.15	28 days, room temperature	2 MPa, 7 h
GP-3	65	0.15	28 days, room temperature	2 MPa, 7 h
GP-4	50	0.15	28 days, room temperature	2 MPa, 7 h

The mixtures had to be mixed for at least 30 minutes to ensure the powder dissolved into the NaOH solution. We poured the sludge into 80 mm long, 40 mm wide, and 20 mm high molds. Then, we compressed the sample with a pressing speed of 1 MPa/s and forming pressure of 3.5 MPa using Technotech experimental press. The sample's weight was about 70 gr (Fig.1). We divided these green samples into two groups. The first group was cured in an autoclave at a pressure of 2 MPa and temperature of about 215 ºC for 7 hours. The second group was cured at room temperature for 28 days. The series for the compressive strength test comprised three specimens.

Figure 1. Geopolymer samples.

2.4. Methods of analysis

Inductively coupled plasma mass spectrometry (ICP-MS) was used to determine the activated silica and alumina. In this case, the 2.5 g of WTR and CFA were digested with 25 mL of the 8M NaOH solution in screw-top PTFE-lined stainless-steel bombs at (80 ± 2) °C for 24 hours following filtrate through a 25 mm filter.

We used Bruker/Siemens D5000 automated X-ray powder diffractometer to analyze the composition of raw materials and geopolymers. The XRD analysis used CuK radiation with a step size of 0.02°, a scan speed of 0.02° per 2 s, and a scan range of 10–55 2theta (diffraction angle). We also used FEI Quanta 200 Scanning Electron Microscope (SEM) at an accelerating voltage of 20 kV to examine the morphologies and microstructure of the materials.

The bonding interactions of raw materials and geopolymers were analyzes based on a Fourier Transform Infrared (FTIR) Spectrum using a spectrometer set Nicolet 6700 with scan frequencies range of 400–2000 cm^{-1}.

A compression testing machine (Tecnotest of Via DelleIndustrie, Inc., Italy) was used to determine the unconfined compressive strength of geopolymer specimens. The strain rate was 1.5% per minute. We polished two specimen's ends with sandpaper to meet the requirements on flatness and perpendicularity. Then, we applied a thin oil layer on the two specimen's ends to reduce the friction and the shear stress between the surfaces of the plates and the specimen.

3. Results and Discussions

3.1. XRD analysis

The XRD patterns of WTR, CFA, and GP-1 (normal and autoclave curing) are shown in Fig 2.

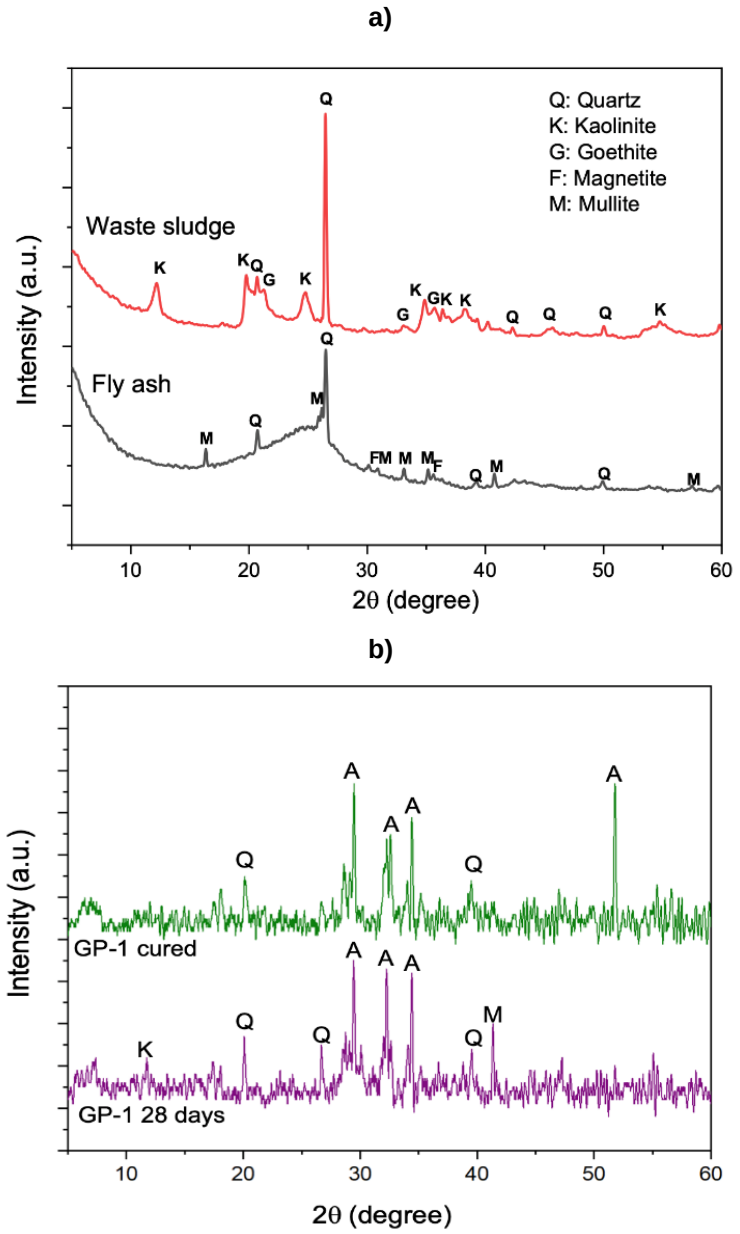

Figure 2. XRD patterns of CFA and WTR (a); GP-1 normally cured for 28 days, GP-1 autoclave cured for 7 hours (b).

The characteristic peaks of mullite (M), goethite (F), kaolinite (K), and quartz (Q) are visible on XRD patterns of WTR and CFA (Fig. 2a). These peaks disappeared on XRD patterns of GP-1 (normal and autoclave curing). The intensity of Q characteristic peaks is significantly reduced (Fig. 2b).

The results are evidence of the geopolymer formation based on WTR and CFA. In Fig. 2b, the analcime characteristic peaks (A) of zeolite are visible on XRD patterns of GP-1 specimens. The results also reveal that autoclave curing can improve the relative crystallinity of analcime zeolite. After 7 hours of curing in an autoclave under 2 MPa pressure, the relative crystallinity is better than after 28 days of curing in normal conditions.

3.1. FTIR analysis

The FTIR spectra of WTR, CFA, and GP-1 (normal and autoclave curing) are shown in Fig 3.

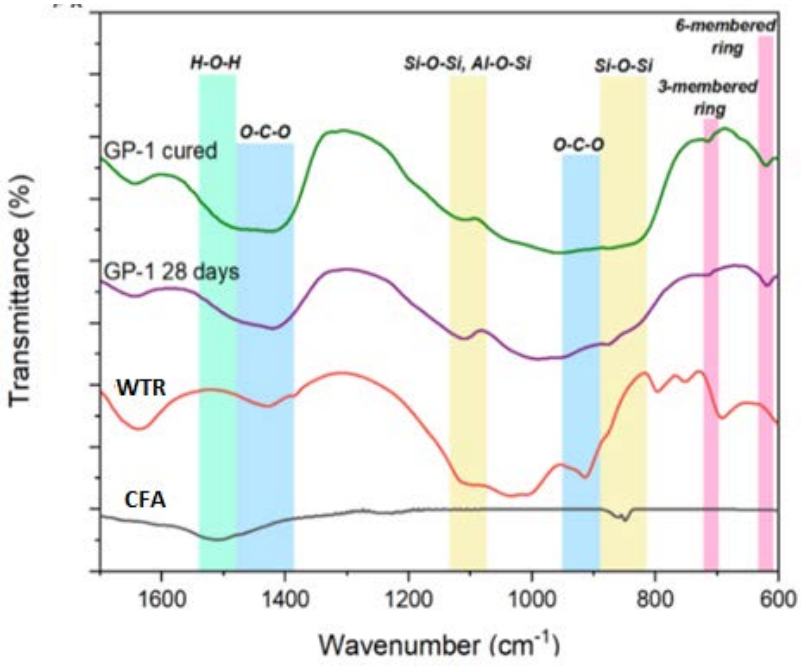

Figure 3. FTIR spectra of CFA, WTR, and GP-1 (normal and autoclave curing).

The vibrations in the 850–1200 cm^{-1} range on the FTIR spectra indicate the footprint of geopolymer bonds. The distribution of SiQ^n structural units has to be reflected by the broadness of this band. It is well known that the stretching vibrations of the –Si–O–Si– bonds of the SiQ^n structural units are FTIR active in the 850–1200 cm^{-1} range. The FTIR absorption band centered around 1200 cm^{-1}, 1100 cm^{-1}, 950 cm^{-1}, 900 cm^{-1}, and 850 cm^{-1} show the presence of the SiQ^4, SiQ^3, SiQ^2, SiQ^1, and SiQ^0 units, respectively. These values shift to lower wavenumbers when the degree of silicon substitution by aluminum in the second coordination sphere increases due to the weaker Al-O bonds [35].

In Fig. 3, the FTIR spectra showed a maximum absorption band in the range of 1050–1150 cm^{-1}, consistent with the predominance of SiQ^3 and SiQ^4 structural units over SiQ^0, SiQ^1, and SiQ^2 ones. The FTIR spectra also show the systematic shift of the maximum absorption band toward higher wavenumbers in the autoclave-cured geopolymer. It indicates the predominance of the SiQ^4 structural unit over the SiQ^3 in the produced gelatinous silicate phases. The silicon-oxygen ring vibrational bands occur in the wavenumbers region of 500–800 cm^{-1} [36].

In the FTIR spectra, we also can investigate the silicone-oxygen ring vibrational band in the geopolymer specimen. Three-membered and six-membered rings showed sharp peaks at 750–770 cm^{-1} and 600–620 cm^{-1}, respectively. The presence of six-membered rings is a conclusive proof that analcime is viable in geopolymer structures [37]. The sludge specimens are more sensitive to atmospheric carbonation than the geopolymer samples by the displays of carbonate species at 1450 cm^{-1} and 870 cm^{-1}.

3.2. SEM analysis

Fig. 4(a) and Fig. 4(b) show the microstructure of WTR and CFA. Fig. 4(c) and Fig. 4(d) show the microstructure of the geopolymer specimens.

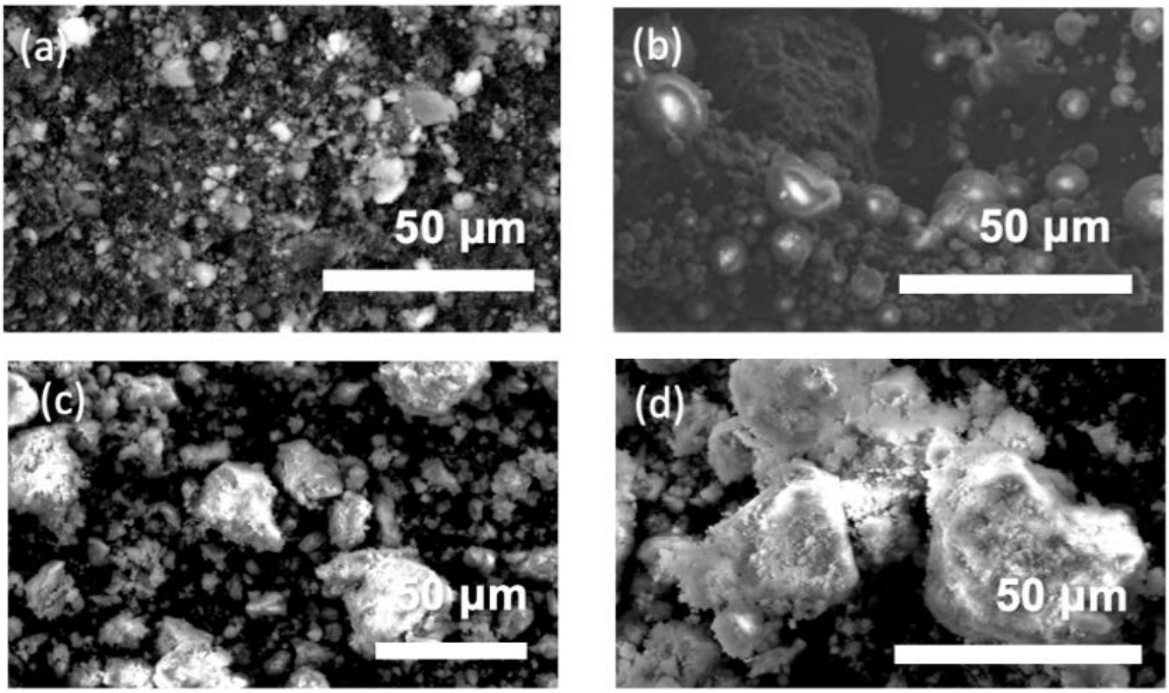

Figure 4. SEM images of WTR (a), CFA (b), normally cured GP-1 (c), and autoclave cured GP-1 (d).

In SEM images in Fig. 4, we can find the WTR particles in the form of irregularly shaped aggregates created by much smaller particles. They are likely hematite particles. The shape of the CFA particles is generally spherical. The regular geopolymer particles are variable in size and have a thin shell or plate-like shape. The WTR and CFA microstructures can help us to identify the originality of some phases (e.g., non-reactive or unreacted reactive phases) in the final products.

The microstructure in SEM images is porous and inhomogeneous with micro-voids and micro-cracks. The formation of voids and cracks may occur due to shrinkage caused by water evaporation, outside load (e.g., compressive testing load), or entrained air bubbles. The analcime zeolite crystals formed in autoclave conditions are coarser than in normal conditions. The crystallization rate depends on the saturation of the solution and the heterogeneous nucleation agents. These agents may be crystalline and amorphous aluminosilicate particles insoluble in the solution [10, 37]. In autoclave conditions, the analcime crystals grew significantly faster and coarser, and therefore the microstructure was more inhomogeneous. This phenomenon implied the critical role of autoclave curing in crystallizing analcime in geopolymer materials.

3.3. Compressive Strength

Fig. 5 shows the compressive strength test results and the calculated SiO_2/Al_2O_3 ratio (based on Table 3 with 8M NaOH solution) of GP-1, GP-2, GP-3, and GP-4 samples under different curing conditions. The results showed that the control specimens with a WTR/CFA ratio of 80 % cured in normal conditions did not harden and did not develop compressive strength. In this case, autoclave curing is essential to stimulate the reaction and increase compressive strength to 7.0 MPa.

Increasing the SiO_2/Al_2O_3 ratio and the content of CFA also improves the compressive strength of geopolymers in both curing conditions. Lowering the WTR/CFA ratio from 80% to 50% increased the SiO_2/Al_2O_3 ratio from 0.49 to 1.79 and the compressive strength from zero to 13.2 MPa (normally cured) and from 7.0 MPa to 28.8 MPa (autoclave cured). Excluding the control specimens, all geopolymers meet the strength requirements for unfired materials following the Vietnam national standard (> 3.5 MPa).

Geopolymers cured in autoclave conditions for 7 hours had higher compressive strength than those cured in normal conditions for 28 days (Fig. 5). These results are clear evidence of the superiority of autoclave technology in forming analcime crystals. The high pressure in the autoclave created a better condition for breaking the bonds in the precursors (WTR, CFA) and the formation of geopolymer structure $Mn[-(SiO_2)_z - AlO_2]_n.mH_2O$.

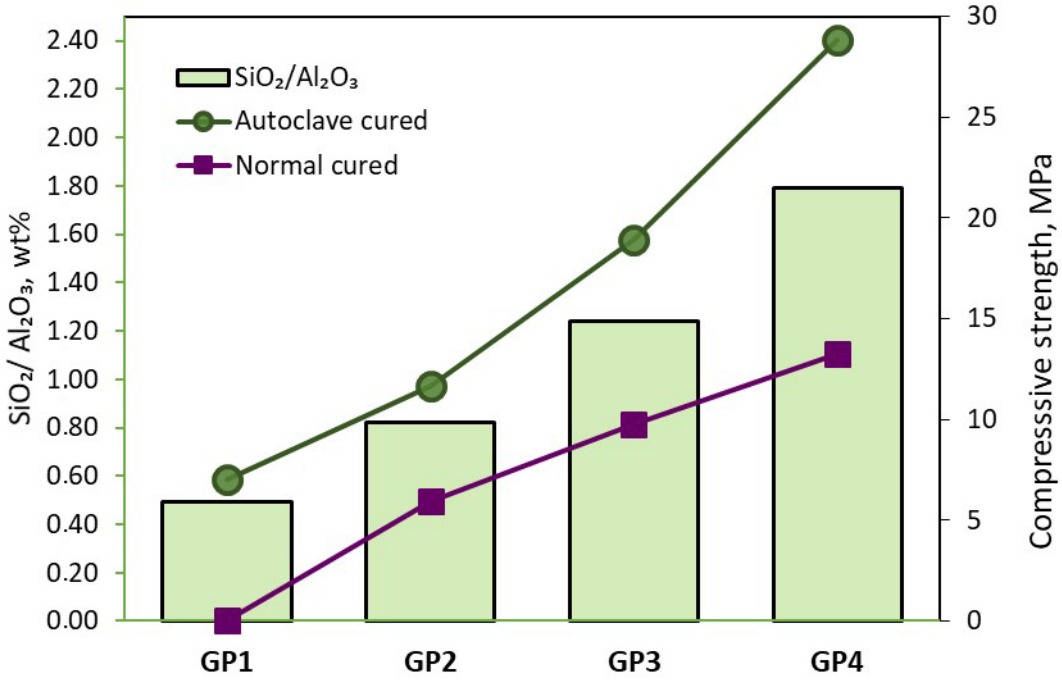

Figure 5. Compressive strength and the active SiO2/Al2O3 ratio under different curing conditions.

4. Conclusions

Geopolymers were successfully synthesized with WTR, CFA, and 8M NaOH solutions by autoclaving at 2 MPa pressure for 7 hours or normal curing in the atmosphere for 28 days. The results showed that the compressive strength of the autoclave cured geopolymer reached 28.8 MPa, which is significantly higher than in those cured in normal conditions (13.2 MPa). Increasing the SiO_2/Al_2O_3 ratio increased the compressive strength of geopolymers in both curing conditions.

The microstructure (XRD, SEM) and chemical bonding (FTIR) analysis confirmed the analcime crystal formation in the geopolymer. Autoclaving is an effective curing technology that improves the geopolymerization and the compressive strength of geopolymers using WTR.

References

1. Benlalla, A., Elmoussaouiti, M., Dahhou, M., Assafi, M. Utilization of water treatment plant sludge in structural ceramics bricks. Applied Clay Science. 2015. 118. Pp. 171–177. DOI:10.1016/j.clay.2015.09.012.
2. Cremades, L. V., Cusidó, J.A., Arteaga, F. Recycling of sludge from drinking water treatment as ceramic material for the manufacture of tiles. Journal of Cleaner Production. 2018. 201. Pp. 1071–1080. DOI:10.1016/j.jclepro.2018.08.094.
3. Ewais, E.M.M., Elsaadany, R.M., Ahmed, A.A., Shalaby, N.H., Al-Anadouli, B.E.H. Insulating Refractory Bricks from Water Treatment Sludge and Rice Husk Ash. Refractories and Industrial Ceramics. 2017. 58(2). Pp. 136–144. DOI:10.1007/S11148-017-0071-6.
4. Teixeira, S.R., Santos, G.T.A., Souza, A.E., Alessio, P., Souza, S.A., Souza, N.R. The effect of incorporation of a Brazilian water treatment plant sludge on the properties of ceramic materials. Applied Clay Science. 2011. 53(4). Pp. 561–565. DOI:10.1016/j.clay.2011.05.004.
5. Erdogmus, E., Harja, M., Gencel, O., Sutcu, M., Yaras, A. New construction materials synthesized from water treatment sludge and fired clay brick wastes. Journal of Building Engineering. 2021. 42. Pp. 102471. DOI:10.1016/J.JOBE.2021.102471.
6. Huang, C.H., Wang, S.Y. Application of water treatment sludge in the manufacturing of lightweight aggregate. Construction and Building Materials. 2013. 43. Pp. 174–183. DOI:10.1016/j.conbuildmat.2013.02.016.
7. Xu, G.R., Zou, J.L., Li, G.B. Effect of sintering temperature on the characteristics of sludge ceramsite. Journal of Hazardous Materials. 2008. 150(2). Pp. 394–400. DOI:10.1016/J.JHAZMAT.2007.04.121.
8. Huang, C.H., Wang, S.Y. Application of water treatment sludge in the manufacturing of lightweight aggregate. Construction and Building Materials. 2013. 43. Pp. 174–183. DOI:10.1016/J.CONBUILDMAT.2013.02.016.
9. Dahhou, M., El Moussaouiti, M., Arshad, M.A., Moustahsine, S., Assafi, M. Synthesis and characterization of drinking water treatment plant sludge-incorporated Portland cement. Journal of Material Cycles and Waste Management. 2018. 20(2). Pp. 891–901. DOI:10.1007/S10163-017-0650-0.
10. Chen, H.X., Ma, X., Dai, H.J. Reuse of water purification sludge as raw material in cement production. Cement and Concrete Composites. 2010. 32(6). Pp. 436–439. DOI:10.1016/j.cemconcomp.2010.02.009.
11. Pan, J.R., Huang, C., Lin, S. Reuse of fresh water sludge in cement making. Water Science and Technology. 2004. 50(9). Pp. 183–188. DOI:10.2166/WST.2004.0566.
12. Ahmad, T., Ahmad, K., Alam, M. Investigating calcined filter backwash solids as supplementary cementitious material for recycling in construction practices. Construction and Building Materials. 2018. 175. Pp. 664–671. DOI:10.1016/J.CONBUILDMAT.2018.04.227.

13. Gastaldini, A.L.G., Hengen, M.F., Gastaldini, M.C.C., Do Amaral, F.D., Antolini, M.B., Coletto, T. The use of water treatment plant sludge ash as a mineral addition. Construction and Building Materials. 2015. 94. Pp. 513–520. DOI:10.1016/j.conbuildmat.2015.07.038.
14. Liu, Y., Zhuge, Y., Chow, C.W.K., Keegan, A., Li, D., Pham, P.N., Huang, J., Siddique, R. Properties and microstructure of concrete blocks incorporating drinking water treatment sludge exposed to early-age carbonation curing. Journal of Cleaner Production. 2020. 261. Pp. 121257. DOI:10.1016/J.JCLEPRO.2020.121257.
15. Sales, A., De Souza, F.R., Almeida, F.D.C.R. Mechanical properties of concrete produced with a composite of water treatment sludge and sawdust. Construction and Building Materials. 2011. 25(6). Pp. 2793–2798. DOI:10.1016/j.conbuildmat.2010.12.057.
16. Godoy, L.G.G. de, Rohden, A.B., Garcez, M.R., Da Dalt, S., Bonan Gomes, L. Production of supplementary cementitious material as a sustainable management strategy for water treatment sludge waste. Case Studies in Construction Materials. 2020. 12. Pp. e00329. DOI:10.1016/J.CSCM.2020.E00329.
17. Geraldo, R.H., Fernandes, L.F.R., Camarini, G. Water treatment sludge and rice husk ash to sustainable geopolymer production. Journal of Cleaner Production. 2017. 149. Pp. 146–155. DOI:10.1016/J.JCLEPRO.2017.02.076.
18. Hwang, C.L., Chiang, C.H., Huynh, T.P., Vo, D.H., Jhang, B.J., Ngo, S.H. Properties of alkali-activated controlled low-strength material produced with waste water treatment sludge, fly ash, and slag. Construction and Building Materials. 2017. 135. Pp. 459–471. DOI:10.1016/J.CONBUILDMAT.2017.01.014.
19. Ji, Z., Pei, Y. Geopolymers produced from drinking water treatment residue and bottom ash for the immobilization of heavy metals. Chemosphere. 2019. 225. Pp. 579–587. DOI:10.1016/J.CHEMOSPHERE.2019.03.056.
20. Nimwinya, E., Arjharn, W., Horpibulsuk, S., Phoo-Ngernkham, T., Poowancum, A. A sustainable calcined water treatment sludge and rice husk ash geopolymer. Journal of Cleaner Production. 2016. 119. Pp. 128–134. DOI:10.1016/J.JCLEPRO.2016.01.060.
21. Suksiripattanapong, C., Horpibulsuk, S., Chanprasert, P., Sukmak, P., Arulrajah, A. Compressive strength development in fly ash geopolymer masonry units manufactured from water treatment sludge. Construction and Building Materials. 2015. 82. Pp. 20–30. DOI:10.1016/j.conbuildmat.2015.02.040.
22. Waijarean, N., MacKenzie, K.J.D., Asavapisit, S., Piyaphanuwat, R., Jameson, G.N.L. Synthesis and properties of geopolymers based on water treatment residue and their immobilization of some heavy metals. Journal of Materials Science. 2017. 52(12). Pp. 7345–7359. DOI:10.1007/S10853-017-0970-4.
23. Provis, J.L. Alkali-activated materials. 114. Elsevier Ltd, 01-12-2018.
24. Davidovits, J. Geopolymer - Chemistry and Application2015. ISBN:9782954453118.
25. Davidovits, J. Geopolymers: ceramic-like inorganic polymers. Journal of Ceramic Science and Technology. 2017. 8(3). Pp. 335–350. DOI:10.4416/JCST2017-00038.
26. He, Y., Cui, X. min, Liu, X. dong, Wang, Y. pin, Zhang, J., Liu, K. Preparation of self-supporting NaA zeolite membranes using geopolymers. Journal of Membrane Science. 2013. 447. Pp. 66–72. DOI:10.1016/J.MEMSCI.2013.07.027.
27. MacKenzie, K.J.D., Brew, D.R.M., Fletcher, R.A., Vagana, R. Formation of aluminosilicate geopolymers from 1:1 layer-lattice minerals pre-treated by various methods: a comparative study. Journal of materials science. 2007. 42(12). Pp. 4667–4674. DOI:doi.org/10.1007/s10853-006-0173-x.
28. Ge, Y.Y., Tang, Q., Cui, X.M., He, Y., Zhang, J. Preparation of large-sized analcime single crystals using the Geopolymer-Gels-Conversion (GGC) method. Materials Letters. 2014. 135. Pp. 15–18. DOI:10.1016/J.MATLET.2014.07.122.
29. Kupwade-Patil, K., Allouche, E.N. Impact of alkali silica reaction on fly ash-based geopolymer concrete. Journal of Materials in Civil Engineering. 2015. 25(1). Pp. 131–139. DOI:10.1061/(ASCE)MT.1943-5533.0000579.
30. Provis JL and Van Deventer JSJ. Geopolymers: Structure, Processing, Properties and Industrial Applications. CRC/Woodhead, 2009.
31. Duxson, P., Provis, J.L. Designing precursors for geopolymer cements. Journal of the American Ceramic Society. 2008. 91. Pp. 3864–3869. DOI:10.1111/j.1551-2916.2008.02787.x.
32. Waijarean, N., Asavapisit, S., Sombatsompop, K., MacKenzie, K.J.D. The Effect of the Si/Al Ratio on the Properties of Water Treatment Residue (WTR)-Based Geopolymers. Key Engineering Materials. 2014. 608. Pp. 289–294. DOI:10.4028/www.scientific.net/KEM.608.289.
33. Suksiripattanapong, C., Srijumpa, T., Horpibulsuk, S., Sukmak, P., Arulrajah, A., Du, Y.J. Compressive strengths of water treatment sludge-fly ash geopolymer at various compression energies. Lowland Technology International. 2017. 17(3). Pp. 147–156. DOI:10.14247/lti.17.3_147.
34. Hoang, M.D., Do, Q.M., Le, V.Q. Effect of curing regime on properties of red mud based alkali activated materials. Construction and Building Materials. 2020. 259. Pp. 119779. DOI:10.1016/j.conbuildmat.2020.119779.
35. Dimas, D., Giannopoulou, I., Panias, D. Polymerization in sodium silicate solutions: a fundamental process in geopolymerization technology. Journal of Materials Science. 2009. 44(14). Pp. 3719–3730. DOI:10.1007/s10853-009-3497-5.
36. Lecomte, I., Henrist, C., Liegeois, M., Maseri, F., Rulmont, A., Cloots, R. (Micro) structural comparison between geopolymers, alkali-activated slag cement and Portland cement. Journal of the European Ceramic Society. 2006. 26(16). Pp. 3789–3797. DOI:10.1016/j.jeurceramsoc.2005.12.021.
37. Sitarz, M., Handke, M., Mozgawa, W. Identification of silico oxygen rings in SiO2 based on IR spectra. SpectrochimicaActa Part A: Molecular and Biomolecular Spectroscopy. 2020. 56(9). Pp. 1819–1823. DOI:10.1016/S1386-1425(00)00241-9.
38. Itani, L., Liu, Y., Zhang, W., Bozhilov, K.N., Delmotte, L., Valtchev, V. Investigation of the physicochemical changes preceding zeolite nucleation in a sodium-rich aluminosilicate ge. Journal of the American Ceramic Society. 2009. 131(29). Pp. 10127–10139. DOI:10.1021/ja902088f.

Contacts:

Quang Minh Do, *PhD*
ORCID: https://orcid.org/0000-0001-5714-1259
E-mail: mnh_doquang@hcmut.edu.vn

Huynh Uyen Phuong Nguyen,
ORCID: https://orcid.org/0000-0002-7256-4097
E-mail: phuongup@gmail.com

Van Quang Le, *PhD*
ORCID: https://orcid.org/0000-0003-0922-9891
E-mail: quanghuce83@gmail.com

Minh Duc Hoang, *PhD*
ORCID: https://orcid.org/0000-0001-8413-8741
E-mail: hmduc@yahoo.com

Received 27.11.2020. Approved after reviewing 11.02.2022. Accepted 15.02.2022.